Kidney360

Molecular Phenotyping and Mechanisms of Myocardial Fibrosis in Advanced Chronic Kidney Disease

Gayatri Narayanan,[1] Arvin Halim,[1] Alvin Hu,[1,2] Keith G. Avin,[1,3] Tzongshi Lu,[4] Daniel Zehnder,[5] Takashi Hato,[1] Neal X. Chen,[1] Sharon M. Moe,[1] and Kenneth Lim[1]

Key Points

- Myocardial fibrosis in hearts from patients with CKD is characterized by increased trimeric tensile collagen type I and decreased elastic collagen type III compared with hearts from hypertensive or healthy donors, suggesting a unique fibrotic phenotype.
- Myocardial fibrosis in CKD is driven by alterations in extracellular matrix proteostasis, including dysregulation of metalloproteinases and cross-linking enzymes.
- CKD-associated mineral stressors uniquely induce a fibronectin-independent mechanism of fibrillogenesis characterized by formation of trimeric collagen compared with proinflammatory/fibrotic cytokines.

Abstract

Background Myocardial fibrosis is a major life-limiting problem in CKD. Despite this, the molecular phenotype and metabolism of collagen fibrillogenesis in fibrotic hearts of patients with advanced CKD have been largely unstudied.

Methods We analyzed explanted human left ventricular (LV) heart tissues in a three-arm cross-sectional cohort study of deceased donor patients on hemodialysis (HD, $n=18$), hypertension with preserved renal function (HTN, $n=8$), and healthy controls (CON, $n=17$), *ex vivo*. RNA-seq and protein analysis was performed on human donor hearts and cardiac fibroblasts treated with mineral stressors (high phosphate and high calcium). Further mechanistic studies were performed using primary cardiac fibroblasts, *in vitro* treated with mineral stressors, proinflammatory and profibrotic cytokines.

Results Of the 43 donor participants, there was no difference in age ($P > 0.2$), sex ($P > 0.8$), or body mass index ($P > 0.1$) between the groups. Hearts from the HD group had extensive fibrosis ($P < 0.01$). All LV tissues expressed only the trimeric form of collagen type I. HD hearts expressed increased collagen type I ($P < 0.03$), elevated collagen type I:III ratio ($P < 0.05$), and decreased MMP1 ($P < 0.05$) and MMP2 ($P < 0.05$). RNA-seq revealed no significant differential gene expression of extracellular matrix proteins of interest in HD hearts, but there was significant upregulation of LH2, periostin, α-SMA, and TGF-β1 gene expression in mineral stressor–treated cardiac fibroblasts. Both mineral stressors ($P < 0.009$) and cytokines ($P < 0.03$) increased collagen type I:III ratio. Mineral stressors induced trimeric collagen type I, but cytokine treatment induced only dimeric collagen type I in cardiac fibroblasts. Mineral stressors downregulated fibronectin ($P < 0.03$) and MMP2 zymogen ($P < 0.01$) but did not significantly affect expression of periostin, MMP1, or cross-linking enzymes. TGF-β upregulated fibronectin ($P < 0.01$) and periostin ($P < 0.02$) only.

Conclusions Myocardial fibrosis in advanced CKD hearts is characterized by increased trimeric collagen type I and dysregulated collagen metabolism, and is differentially regulated by components of uremia.

KIDNEY360 4: 1562–1579, 2023. doi: https://doi.org/10.34067/KID.0000000000000276

[1]Division of Nephrology and Hypertension, Indiana University School of Medicine, Indianapolis, Indiana
[2]Department of Medicine, Indiana University Health Ball Memorial Hospital, Indianapolis, Indiana
[3]Department of Physical Therapy, Indiana University School of Health and Human Sciences, Indiana University, Indianapolis, Indiana
[4]Renal Division, Brigham and Women's Hospital, Harvard Medical School, Boston, Massachusetts
[5]Department of Nephrology and Department of Acute Medicine, North Cumbria University Hospital NHS Trust, Carlisle, United Kingdom

Correspondence: Dr. Kenneth Lim, Division of Nephrology and Hypertension, Indiana University School of Medicine, 950 West Walnut Street, R2 E221, Indianapolis, IN 46202. Email: kjlim@iu.edu

Introduction

Myocardial fibrosis is a major complication in patients with CKD that can develop early in the progression of CKD.[1–4] Myocardial fibrosis is the abnormal excess deposition of extracellular matrix (ECM) proteins within the myocardium and can lead to myocardial stiffness,[5–7] diastolic failure,[7–9] increased risk of arrythmias,[10–12] and sudden cardiac death and mortality.[13,14] Reactive myocardial fibrosis is the most common pattern of myocardial fibrosis in CKD and is characterized by the excessive deposition of ECM proteins in the interstitial space because of volumetric, inflammatory, and hormonal (*i.e.*, PTH or FGF23) factors independent of cardiomyocyte loss.[1,3,8,15–18]

The ECM is composed of a complex interactive mixture of proteoglycans, glycosaminoglycans, and glycoproteins secreted by cardiac fibroblasts that serve structural and nonstructural functions.[19–24] Balance of the ECM composition is essential to maintain structural and functional integrity of the myocardium.[25] In healthy myocardium, the ECM is predominantly composed of 80%–85% collagen type I required for tensile strength and 11%–20% collagen type III for elasticity.[26,27] However, in patients with CKD, an increased ratio of collagen type I:III characteristic of fibrosis occurs in the myocardial wall. Moreover, the formation of pathologic trimeric collagen with greater cross-linking has been shown to lead to altered mechanical properties in patients with non-CKD ischemic cardiomyopathy, resulting in diastolic dysfunction.[28,29] Despite the significant burden of myocardial fibrosis in patients with kidney failure, whether pathologic collagen trimerization occurs in fibrillogenesis of the failing heart in CKD and the molecular mechanisms involved in collagen metabolism is largely unknown.

In addition, the production of collagen fibers, which is referred to as fibrillogenesis, is also regulated by a fine balance of matrix metalloproteinases (MMPs), tissue inhibitors of metalloproteinases (TIMPs),[30–34] and critical and auxiliary ECM proteins, such as fibronectin and periostin.[35–40] However, to date, few studies have examined the role of these regulators, their regulation, and metabolism of collagen at the heart in advanced CKD. Therefore, the overall goal of this study was to determine the molecular phenotype of collagen matrix formation, define alterations in its regulatory enzymes, and determine the role of uremic components in driving this process. We hypothesize that hearts from patients with advanced CKD on hemodialysis exhibit a distinct molecular pattern in collagen matrix formation and matricellular protein expression, including increased collagen I:III ratio, fibronectin, and cross-linking enzymes compared with hearts from healthy patients and patients with only hypertension. In this study, we demonstrated that myocardial fibrosis in CKD is (*1*) characterized by trimeric collagen formation involving defects in the regulation of MMPs, cross-linking enzymes, and other matricellular proteins; (*2*) this occurs through a fibronectin-independent mechanism of collagen fibrillogenesis and (*3*) is driven largely by abnormal mineral metabolism in CKD rather than proinflammatory/fibrotic cytokines.

Methods

Human Heart Studies

We examined explanted human heart samples that were collected as part of the CAIN (Cardiac Aging in CKD) cohort as previously described.[41] In brief, the CAIN study collected 109 deceased donor hearts. Hearts were obtained through the National Disease Research Interchange (NDRI) from donor participants that were not transplanted and had donated organs for research purposes. In this study, we performed a three-arm cross-sectional study of donor left ventricular (LV) heart tissues from a total of 43 patients with CKD stage 5 on hemodialysis (HD, $n=18$), those who had essential primary hypertension (HTN, $n=8$), and healthy deceased donors without a history of cardiovascular, renal, or metabolic diseases (CON, $n=17$). We performed a three-group comparison of baseline demographic variables (Table 1) and laboratory values (Table 2). We then performed two-group comparisons with our assessments of LV heart tissue, *ex vivo*. Given that our primary group of interest were heart samples from HD donors, we focused on comparing (*1*) HD versus CON to assess the disease effect of advanced CKD and (*2*) HD versus HTN to delineate the effects of hypertension from the other effects of CKD given that hypertension is highly prevalent in the population with CKD. We also compared HTN versus CON to assess the disease effect of hypertension as part of our secondary analysis. Exclusion criteria included deceased donors who were on peritoneal dialysis, patients who had a history of AKI, or those with degraded samples.

Clinical and demographic data were recorded from data provided by the NDRI. Donors were assessed for comorbidities, including history of diabetes and cardiovascular disease. Kidney function was determined by the CKD-Epidemiology Collaboration (CKD-EPI) equation for eGFR.[42,43] Baseline laboratory measures were collected from donors before organ harvesting. Organs were freshly harvested, transported on ice, and underwent pathologic gross examination. Hearts were excised into separate anatomic sections and stored in −80°C. LV sections were either formalin-fixed to generate paraffin-embedded sections or snap frozen. Snap frozen LV blocks were manually homogenized, sonicated, and solubilized for RNA isolation using the RNeasy Mini Kit (Cat. No. 74104; Qiagen, Germantown, MD), and protein isolation was performed using radioimmunoprecipitation assay (RIPA) buffer (Cat. No. BP-115; Boston BioProducts, Ashland, MA). This study qualified for Indiana University IRB exemption (Protocol #2006398198) because of secondary analysis of existing biospecimens.

Histological Analysis

Cardiac left ventricular (LV) wall samples from each group were prepared as 6-μm-thick, formalin-fixed paraffin-embedded tissue sections. Masson's trichrome blue staining was used to assess the relative extent of fibrosis or collagen deposition between CON, HTN, and HD LV walls and to test the hypothesis that HD LV walls had greater fibrosis than HTN and CON LV walls. For hematoxylin and eosin staining, tissue sections were automatically processed

Table 1. Baseline characteristics and demographics of study population

Variable	Overall Sample Size	Hemodialysis (HD)	Hypertension (HTN)	Control (CON)	*P* Value
Participants (Total), *n*	43	18	8	17	—
Male (sex), *n* (%)	43	11 (61.11%)	5 (62.50%)	9 (52.94%)	0.86
Race, *n* (%)					
Asian	43	0 (0%)	1 (12.50%)	1 (5.88%)	—
Black		7 (38.89%)	2 (25.00%)	3 (17.65%)	
White		11 (61.11%)	5 (62.50%)	13 (76.47%)	
Ethnicity, *n* (%)					
Hispanic	40	3 (17.65%)	1 (14.29%)	2 (12.50%)	0.92
Non-Hispanic		14 (82.35%)	6 (85.71%)	14 (87.50%)	
Age, yr	43	46.39±11.3	54.5±4.21	50.88±14.57	0.25
BMI, kg/m^2	42	26.78±4.57	30.97±6.27	26.94±6.33	0.19
Smoking, *n* (%)	41	7 (38.89%)	3 (37.50%)	7 (46.67%)	0.87
Comorbidities					
Hypertension, *n* (%)	41	17 (94.44%)	8 (100%)	0 (0%)	0.5[a]
Diabetes, *n* (%)	41	13 (72.22%)	0 (0%)	0 (0%)	<0.0007[a,b]
Coronary artery disease, *n* (%)	41	6 (33.33%)	1 (12.85%)	0 (0%)	0.27[a]
Previous cardiovascular disease event, *n* (%)	22	8 (53.33%)	1 (14.29%)	0 (0%)	0.083[a]
Medications					
ACEi or ARB, *n* (%)	30	5 (41.67%)	1 (14.29%)	0 (0%)	0.22[a]
Statin, *n* (%)	30	6 (50.00%)	1 (14.29%)	0 (0%)	0.12[a]
β-Blocker, *n* (%)	30	6 (50.00%)	0 (0%)	0 (0%)	0.024[a,b]
Aspirin, *n* (%)	29	2 (18.18%)	1 (14.29%)	0 (0%)	0.83[a]
Blood thinner, *n* (%)	29	0 (0%)	0 (0%)	0 (0%)	—

Data are presented as frequency (percentage), mean±SD, or median (interquartile range). *P* values were obtained by one-way ANOVA with *post hoc* Tukey-Kramer HSD for multigroup comparisons of noncategorical variables, and Pearson chi-square for two- and three-group comparisons of categorical variables. BMI, body mass index; ACEi, angiotensin-converting enzyme inhibitor; ARB, angiotensin II receptor blocker.
[a]Two-group comparison between HD and HTN groups with the chi-square test.
[b]*P* value reached significance of < 0.05.

using the LINISTAIN GLX Linear Stainer with Harris' Hematoxylin (Cat. No. 01560; Surgipath, Richmond, IL) and Eosin (Cat. No. 01600; Surgipath, Richmond, IL) solutions. For Masson's trichrome staining, tissue sections were incubated in Biebrich scarlet–acid fuchsin and Weigert's iron hematoxylin solution for 10–15 minutes, followed by incubation in phosphomolybdic-phosphotungstic acid solution for another 10–15 minutes. Tissue sections were then transferred directly and incubated in aniline blue solution for 5–10 minutes. Tissue sections were rinsed in distilled water and differentiated for 2–5 minutes in 1% acetic acid. Blue staining coverage was used as a surrogate measurement for severity of fibrosis and was quantified by ImageJ.

RNA Sequencing Data Analysis

To test the hypothesis that there are differences in fibrotic markers on the transcriptomic level caused by CKD in LV heart tissue or caused by mineral stressors in cardiac fibroblasts, we performed a secondary analysis of RNA sequencing (RNA-seq) data for human LV heart tissue from HD and CON groups and primary human cardiac fibroblasts with or without treatment of mineral stressors. RNA-seq data were downloaded from the NCBI Gene Expression Omnibus database (GEO GSE160145) and processed similarly with edgeR as described previously.[41] All eight HTN, five HD, and 12 CON human LV heart samples were removed from final analysis because of poor sample quality or low read count and batch effects, resulting in only five CON and 13 HD hearts included in the final RNA-seq analysis. Counts data from the GEO repository were normalized and converted to counts per million. Genes with sufficiently large counts for downstream statistical analysis were selected and kept by filterByExpr. Differential gene expression analysis was performed with glmQLFTest and estimateDisp. For human LV heart samples, differential gene expression analysis accounted for sample group, sequencing batch, and sex of sample donor (model.matrix((approximately 0+groupfactor+batchfactor+sexfactor)). For cardiac fibroblasts, differential gene expression analysis accounted for sample group only (model.matrix((approximately 0+groupfactor)). In multiple comparisons, *P* values were adjusted with the false discovery rate method (p.adjust(data, "fdr")). An FDR <0.05 was considered statistically significant. MA plots were designed using ggplot2 and ggrepel. RStudio version 2022.02.1+461 "Prairie Trillium" was used to execute all data analyses and visualization.

Cardiac Fibroblast Cell Culture

Commercially available human ventricular cardiac fibroblasts (Lot 20TL356511, Cat. No. CC-2905; Lonza Bioscience, Walkersville, MA; Cat. No. 6310; ScienCell Research Laboratories, Carlsbad, CA) were cultured in a 5% CO_2/37°C incubator and grown in FGM-3 Cardiac

Table 2. Baseline laboratory values of study population

Variable	Overall Sample Size	Hemodialysis (HD)	Hypertension (HTN)	Control (CON)	*P* Value
Biochemistry					
Sodium, mmol/L	33	138.54±7.57	141.17±2.64	140.21±4.95	0.62
Potassium, mmol/L	33	5.03±1.07	3.6±0.46	3.31±0.78	<0.0001[a]
Bicarbonate, mmol/L	33	24.02±7.09	24.38±4.59	22.00±3.37	0.53
Blood urea nitrogen, mmol/L	33	57.92±34.1	17.33±7.74	12.5±5.37	<0.0001[a]
Creatinine, mg/dl	33	—	1.25 (0.7–1.68)	0.80 (0.7–1.03)	—
GFR, ml/min per 1.73 m^2	33	—	64.05 (47.02–140.98)	111.04 (78.46–129.41)	—
Corrected calcium, mg/dl	31	9.09±1.22	8.85±1.39	8.58±1.00	0.55
Phosphate, mg/dl	32	6.2 (5.4–7.35)	3.25 (2.08–3.8)	2.9 (1.95–3.6)	<0.0001[a]
Magnesium, mmol/L	31	2.15 (2.03–2.7)	2.0 (1.8–2.15)	1.9 (1.55–2.05)	0.014[a]
LDH, U/L	17	239 (153–428)	305 (235–2658)	299 (144.01–839)	0.29
Lipase, U/L	27	97.43±134.51	128±144.38	158.93±375.11	0.9
Liver function					
Albumin, g/L	32	3.5 (2.7–4.2)	4.05 (3.05–4.63)	3.6 (3.3–4.1)	0.39
AST, U/L	33	40.46±41.38	82.17±84.10	53.43±48.9	0.31
ALT, U/L	33	36.23±37.02	32.5±17.59	38.43±28.29	0.92
ALP, U/L	33	114.00±45.08	100.67±43.36	69.21±17.16	0.0087[a]
Hematology					
Hemoglobin, g/dl	33	11.1 (9.8–12.65)	14.1 (13.03–17.05)	12.05 (10.98–13.95)	0.018[a]
Hematocrit, %	33	32.50 (30.6–37.3)	41.55 (37.3–50.68)	36.45 (33.05–40.38)	0.017[a]
Platelets, 10^5/L	33	214.54±104.22	211.0±125.77	209.14±84.2	0.99
Cardiac biomarkers					
Troponin T, ng/L	10	0.11±0.15	0.01	0.24±0.5	0.85
Troponin I, ng/L	14	0.74±1.08	0.085±0.063	0.29±0.28	0.43
CPK, U/L	24	156.29±59.78	183.25±93.93	401.23±306.78	0.074
CPK-MB, IU/L	24	5.48±4.93	10.58±12.36	11.88±10.15	0.29

Data are presented as mean±SD or median (interquartile range). *P* values were obtained by one-way ANOVA with *post hoc* Tukey-Kramer HSD for multigroup comparisons of noncategorical variables. LDH, lactate dehydrogenase; AST, aspartate aminotransferase; ALT, alanine transaminase; ALP, alkaline phosphatase; CPK, creatine phosphokinase.
[a]*P* value reached significance of < 0.05.

Fibroblast Growth Medium-3 BulletKit (Cat. No. CC-4526; Lonza Bioscience, Walkersville, MA).

In vitro models of cardiac fibrosis were developed using either mineral stressors or cytokines. For experimental studies, starvation media was supplemented with varying concentrations of β-glycerophosphate disodium salt hydrate (β-GP; Cat. No. G9422; Sigma, St. Louis, MO) and/or calcium chloride ($CaCl_2$; Cat. No. 223506; Sigma, St. Louis, MO) for 10 days for mineral stressor experiments. All treatments containing β-GP also contained 1 unit/ml alkaline phosphatase (ALP, Calf Intestinal; Cat. No. M1821; Promega Corporation, Madison, WI) in the media to hydrolyze β-GP and release phosphate. Starvation media was also supplemented with varying concentrations of tumor necrosis factor-α (*E.coli*-derived human TNF-α, Cat. No. 210-TA/CF; R&D Systems, Minneapolis, MN) or transforming growth factor-β (recombinant human TGF-β, Cat. No. 100-21; PeproTech, Cranbury, NJ) for 5 days for proinflammatory and profibrotic cytokine experiments, respectively. Starvation media treatments were administered daily.

Antibodies

All antibodies were prepared in 3% BSA Blocking Buffer in PBS with 0.02% sodium azide (Cat. No. J60473.AK; Thermo Fisher Scientific, Waltham, MA). COL1A1 [E8I9Z] (Cat. No. 91144; Cell Signaling Technology, Danvers, MA), collagen III [EPR17673] (Cat. No. ab184993; Abcam, Cambridge, United Kingdom), α-smooth muscle actin [Clone 1A4] (Cat. No. A5228; Sigma-Aldrich, St. Louis, MO), fibronectin (Cat. No. ab2413; Abcam, Cambridge, United Kingdom), periostin [EPR19936] (Cat. No. ab219057; Abcam, Cambridge, United Kingdom), LOX [EPR4025, proenzyme] (Cat. No. ab174316; Abcam, Cambridge, United Kingdom), LOX [mature] (Cat. No. 17958-1-AP; Proteintech, Rosemont, IL), lysyl hydroxylase 2 [PLOD2] (Cat. No. 44709; Cell Signaling Technology, Danvers, MA), MMP1 (Cat. No. ab38929; Abcam, Cambridge, United Kingdom), MMP2 [6E3F8] (Cat. No. ab86607; Abcam, Cambridge, United Kingdom), MMP9 [EP1254] (Cat. No. ab76003; Abcam, Cambridge, United Kingdom), and GAPDH [14C10] (Cat. No. 2118; Cell Signaling Technology, Danvers, MA) were utilized for the study.

Statistical Analysis

Clinical demographic information is expressed as frequency (%), mean±SD, or median (interquartile range) as appropriate. Results are expressed as mean and SD or median and interquartile range with upper and lower extremes. Two group comparisons were performed using paired *t* test with unequal variances. Multigroup comparisons were performed using one-way ANOVA or chi-square

tests as appropriate. Statistical analysis and graphing were conducted with JMP Pro (version 16.0.0). Probability values of <0.05 were considered statistically significant.

Supplementary Methods

Detailed descriptions for immunoblotting, cell culturing, and Sircol Insoluble (Cat. No. S2000; Biocolor, Carrickfergus, UK) and Soluble (Cat. No. S1000; Biocolor, Carrickfergus, UK) collagen assays are provided in the Supplemental Methods.

Results

Baseline Characteristics of Study Population

A total of 43 donor hearts were included in this study: 18 patients on hemodialysis (HD), eight patients with essential hypertension (HTN), and 17 healthy controls (CON) (Table 1). Patients on HD were younger and patients with HTN were older compared with CON, but this difference was not significant ($P = 0.25$). There was also no significant difference in sex ($P = 0.86$) or body mass index ($P = 0.19$) across the three groups. A majority of patients on HD had diabetes, which is expected because the high prevalence of diabetic kidney disease. A history of β-blocker use was present only in patients on HD ($P = 0.024$). There was no statistical significance in the use of other cardiac medications between the HD and HTN groups ($P > 0.05$). Patients on HD had higher potassium (HD: 5.03±1.07; HTN: 3.6±0.46; CON: 3.31±0.78 mmol/L; $P < 0.0001$), blood urea nitrogen (HD: 57.92±34.1 mmol/L; HTN: 17.33±7.74 mmol/L; CON: 12.5±5.37 mmol/L; $P < 0.0001$), phosphate (HD: 6.20 [5.40–7.35] mg/dl; HTN: 3.25 [2.08–3.8] mg/dl; CON: 2.90 [1.95–3.60] mg/dl; $P < 0.0001$), and magnesium (HD: 2.15 [2.03–2.70] mmol/L; HTN: 2 [1.8–2.15] mmol/L; CON: 1.90 [1.55–2.05] mmol/L; $P < 0.014$) compared with patients with HTN and CON (Table 2).

Heart and Left Ventricular Section Characteristics

HD ($P < 0.0001$) and HTN ($P < 0.002$) hearts had significantly higher total heart weight normalized to body surface area (BSA) compared with CON hearts (Figure 1A). HD ($P < 0.005$) and HTN ($P < 0.02$) hearts also exhibited higher LV wall thickness normalized to BSA compared with CON hearts. There was no significant difference in normalized heart weight nor normalized LV wall thickness between HD and HTN hearts. Hematoxylin and eosin staining revealed disordered myofiber arrangement in HD hearts compared with CON hearts (Figure 1B). Masson's trichrome staining demonstrated greater fibrosis in LV sections of HD hearts (n=13) and HTN hearts (n=7) compared with CON hearts (n=11, $P < 0.001$). However, hearts from patients on HD had generally worse diffuse and perivascular fibrosis as well as disorganized muscle fiber array compared with hearts from patients with HTN.

Molecular Phenotyping of Collagen and Its Regulatory Enzymes in Human Advanced CKD Hearts

We next performed studies to assess the molecular phenotype of fibrosis by assessing the collagen type I:III ratio through immunoblotting (Figure 2A). Interestingly, we observed expression of only trimeric collagen type I at approximately 400 kDa in all human LV heart tissues. HD hearts had significantly increased collagen type I ($P < 0.03$) and decreased collagen type III ($P < 0.05$), resulting in a greater collagen type I:III ratio compared with CON hearts ($P < 0.04$). HTN hearts had increased collagen type I compared with CON hearts ($P < 0.03$), but not compared with HD hearts. However, HTN hearts had increased collagen type III compared with HD hearts ($P < 0.002$). We next assessed for any dysregulation of collagen matrix regulators. There was no significant difference in periostin, fibronectin, nor α-SMA expression across the three groups (Figure 2B). Cross-linking enzyme mature LOX ($P < 0.04$), and collagenases, MMP1 ($P < 0.05$), and MMP2 ($P < 0.05$) were downregulated in HD hearts compared with CON hearts (Figure 2, C and D). There was no significant difference in LH2 or MMP9 across the three groups.

Given there was increased trimeric collagen type I in HD and HTN hearts, we next investigated whether there was a difference in levels of insoluble collagen between HD, HTN, and CON hearts. Using Sircol assays capable of measuring both acid and pepsin soluble along with insoluble collagen, we found no significant differences in proportion of soluble and insoluble collagen relative to tissue sample mass among HD, HTN, and CON hearts (Supplemental Figure 1).

Transcriptomic Profiling of Advanced CKD Human Hearts and Cardiac Fibroblasts

We sought to determine potential differences in expression of major fibrosis-related genes, including the major collagens (collagen type I α1 chain, COL1A1; collagen type III α1 chain, COL3A1), cross-linking enzymes (lysyl oxidase, LOX; lysyl hydroxylase 2, LH2/PLOD2), metalloproteinases (MMP1/2/9), and collagen matrix assembly regulators (periostin, POSN; fibronectin, FN1). Only HD (n=13) and CON (n=5) hearts were included in RNA-seq analysis because of inadequate sample quality or technical batch effects affecting HTN and CON samples. Transcriptomic profiling revealed there was no significant differential gene expression of the major fibrosis-related genes of interest (Figure 3A).

We next sought to further investigate the mechanisms driving the impairment in ECM proteins observed in LV tissues in advanced CKD by conducting RNA-seq analysis on cardiac fibroblasts treated with (n=3) or without (n=3) mineral stressors (5 mM phosphate and 5 mM calcium) for 48 hours (Figure 3B). Mineral stressors resulted in upregulation of periostin (POSTN), LH2 (PLOD2), α-SMA (ACTA2), and TGF-β1 (TGFB1) compared with control (FDR<0.05). There was no significant difference in gene expression of collagen I (COL1A1 and COL1A3 chains), collagen III (COL3A1), fibronectin (FN1), LOX, MMP2, or GAPDH. There were insufficient counts of MMP1 and MMP9.

Mineral Stress Drives Formation of Intramolecular Cross-Linking of Trimeric Collagen in Cardiac Fibroblasts

We treated primary ventricular cardiac fibroblasts with varying concentrations of phosphate (Figure 4) or calcium (Figure 5), and combined high phosphate and calcium (Figure 6), to investigate whether mineral stressors directly

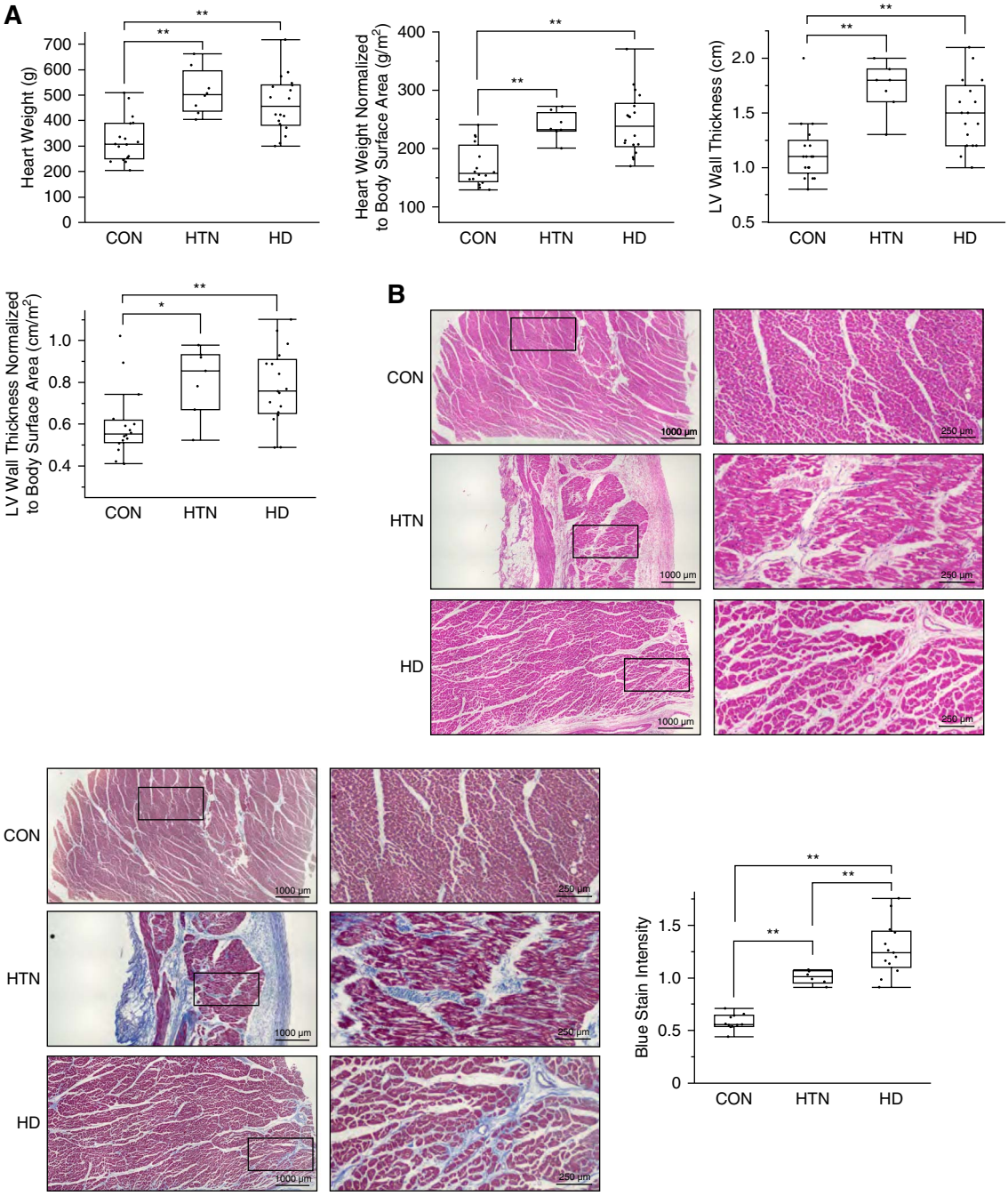

Figure 1. Characteristic of human whole heart and left ventricular sections. Gross characterization and histological analysis of whole and left ventricular human hearts. Representative images utilized 10× (left images) and 20× (right images) objectives. (A) HD and HTN hearts had significantly higher heart weight (HD: $P = 0.0003$, HTN: $P < 0.0001$) and heart weight normalized to BSA (HD: $P < 0.0001$, HTN: $P < 0.0019$) compared with CON hearts. HD and HTN hearts had significantly higher left ventricular (LV) wall thickness (HD: $P = 0.0033$, HTN: $P < 0.0007$) compared with CON hearts. Only HD hearts had significantly higher normalized LV wall thickness to BSA compared with CON hearts ($P < 0.0123$). (B) Hematoxylin and eosin staining of representative left ventricular sections of hearts from a patient on hemodialysis (HD), a patient with hypertension (HTN), and a healthy control donor (CON). HD hearts exhibited disorganized myofibers compared with CON hearts. Masson's trichrome staining of the same tissue sections from the same heart donors. Blue staining represents collagen staining. Quantification of aniline blue stain intensity from Masson's trichrome staining as measurement of fibrosis in hearts from HD (n=13), HTN (n=8), and CON (n=11) donors. P values: *<0.05, **<0.01. Statistical significance determined by one-way ANOVA and pairwise t test.

promote a fibrotic phenotype in cardiac fibroblasts. High phosphate concentrations induced collagen type I trimer expression ($P < 0.02$), increased collagen type I dimers ($P < 0.002$), and decreased collagen type III ($P < 0.006$), overall increasing the total collagen type I:III ratio ($P < 0.05$) compared with control (Figure 4A). High phosphate

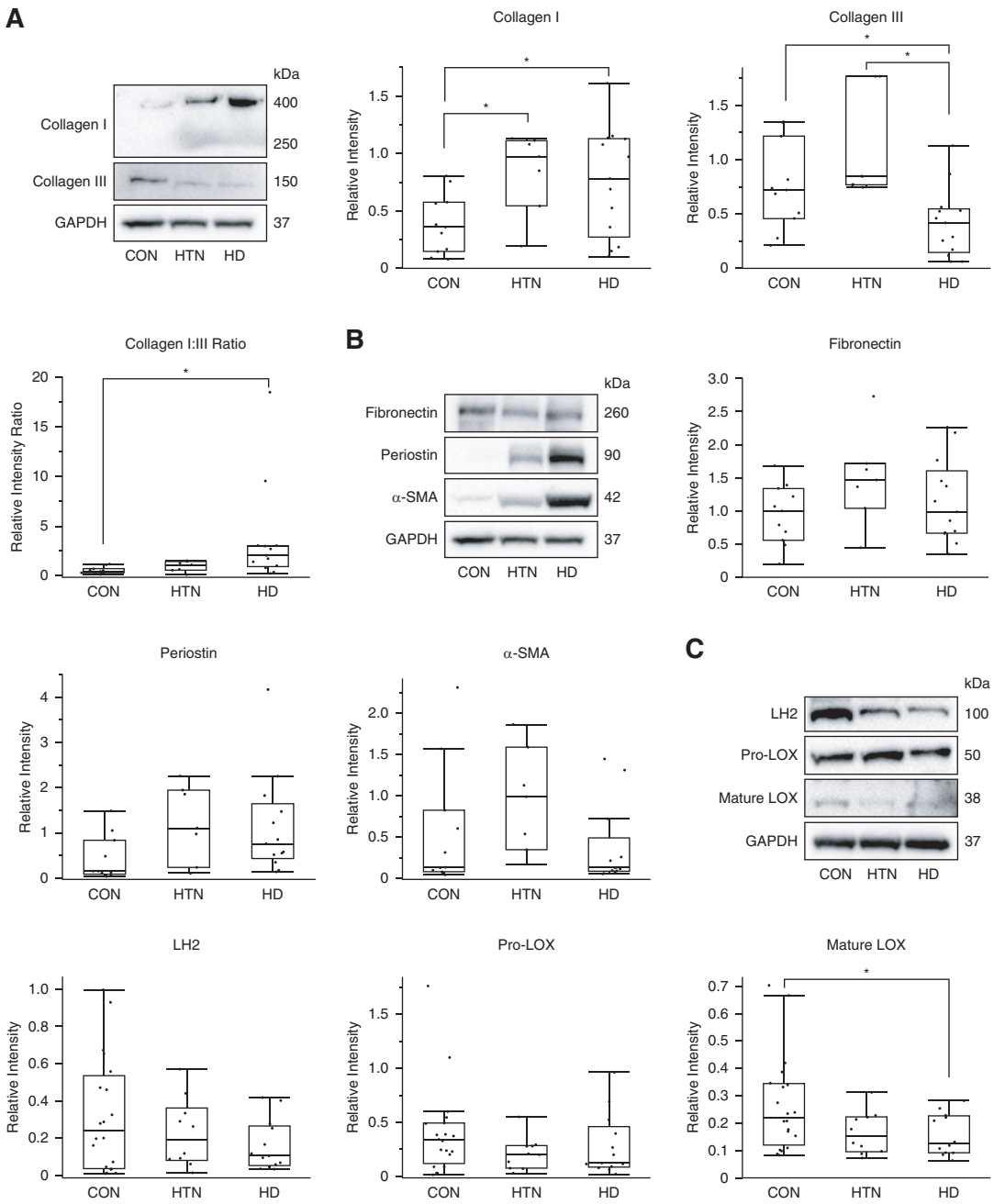

Figure 2. HD hearts exhibit dysregulated collagen synthesis, cross-linking, and turnover. (A) Representative immunoblots of collagen type I, collagen type III, and GAPDH of HD (n=13), HTN (n=8), and CON (n=11) hearts. Trimeric collagen type I appears at 400 kDa, whereas dimeric collagen type I at 250 kDa was not detectable in any group. HD and HTN hearts had a significant increase in collagen type I compared with CON hearts. HD exhibited a significant decrease in collagen type III compared with HTN and CON hearts. HD and HTN hearts had a significantly higher collagen type I/III ratio compared with CON hearts. (B) Representative immunoblots of fibronectin, periostin, α-smooth muscle actin (α-SMA), and GAPDH of HD (n=13), HTN (n=8), and CON (n=11) hearts. There was no significant difference in fibronectin, periostin, and α-SMA expression across all groups. (C) Representative immunoblots of lysyl hydroxylase 2 (LH2), proenzyme lysyl oxidase (pro-LOX), proteolytically processed pro-LOX (mature LOX), and GAPDH of HD (n=13), HTN (n=9), and CON (n=13) hearts. HD hearts had significantly decreased levels of mature LOX compared to CON hearts. There was no significant difference in LH2 and pro-LOX expression across all groups. (D) Representative immunoblots of metalloproteinases 1 (MMP1), 2 (MMP2), and 9 (MMP9), and GAPDH of HD (n=13), HTN (n=9), and CON (n=13) hearts. HD hearts had a significant decrease in MMP1 and MMP2 compared with CON hearts. P values: *<0.05, **<0.01. Statistical significance was determined by one-way ANOVA and pairwise t test.

concentrations also resulted in significant dose-dependent decline in fibronectin ($P < 0.05$) without any significant changes in periostin and α-SMA compared with control (Figure 4B). We also assessed the effect of FBS on phosphate-induced changes in cardiac fibroblasts (Supplemental Figure 2) in cell culture optimization experiments.

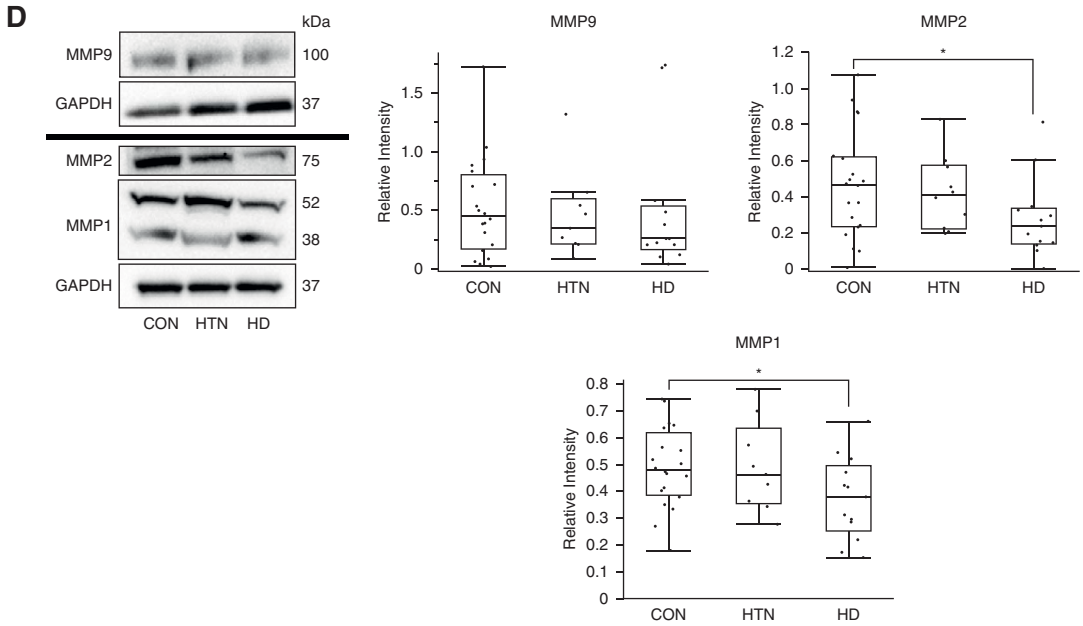

Figure 2. (Continued).

Higher concentrations of FBS significantly increased levels of collagen type I dimers in both high phosphate and control treatments, and levels of collagen type III and fibronectin for high phosphate treatments alone.

Calcium treatments exhibited a similar pattern of extracellular matrix protein expression to phosphate treatments. Collagen type I dimers increased with increasing calcium concentrations up to 4 mM ($P < 0.004$, Figure 5A). We also found that 5 mM calcium significantly drove formation of trimeric collagen type I compared with control ($P < 0.05$). Collagen type III significantly declined when exposed to 5 mM calcium only compared with control ($P < 0.006$). The ratio of total collagen type I:III demonstrated an increasing trend with increasing calcium concentrations, but was only significantly elevated at 5 mM ($P < 0.005$) compared with control (Figure 5B). Fibronectin was significantly downregulated at 4 mM ($P < 0.05$) and further decreased at 5 mM ($P < 0.006$) calcium compared with control.

Combined treatment of 3.8 mM phosphate and 2 mM calcium resulted in a similar increase in trimeric collagen type I ($P < 0.001$), decline in collagen type III ($P < 0.006$), and overall increased total collagen I:III ratio ($P < 0.0002$) compared with 0.9 mM phosphate and 1.8 mM calcium control (Figure 6A). Combined mineral stressors also decreased fibronectin ($P = 0.0002$) but increased α-SMA ($P < 0.03$) and downregulated the zymogen form of MMP2 ($P < 0.01$) compared with control (Figure 6, B–D). There were no significant changes in cross-linking enzymes or other metalloproteinases compared with control.

Proinflammatory and Profibrotic Cytokines Promote Increased Collagen Deposition without Promoting Trimeric Cross-Linked Collagen Formation in Cardiac Fibroblasts

We next assessed whether cytokines, such as TGF-β (Figure 7) and TNF-α (Figure 8), found in CKD would invoke a similar fibrotic molecular phenotype as mineral dysregulation in cardiac fibroblasts. Interestingly, neither TGF-β nor TNF-α treatment resulted in formation of trimeric collagen type I, as seen with mineral stressor treatment. Both TGF-β and TNF-α exhibited a dose-dependent increase in collagen type I and in the ratio of total collagen type I:III with 1–10 ng/ml TGF-β ($P < 0.0002$, Figure 7A) and 5–20 ng/ml TNF-α ($P < 0.0003$, Figure 8A) compared with control. However, only TGF-β resulted in an increasing trend in the expression of collagen type III starting at 1 ng/ml ($P < 0.05$) compared with control. In addition, TGF-β showed dose-dependent increases in fibronectin ($P < 0.01$), periostin ($P < 0.01$), and α-SMA ($P < 0.0003$) starting around 0.5–1 ng/ml compared with control (Figure 7B). Conversely, TNF-α treatments exhibited a significant decrease in α-SMA ($P < 0.0003$) starting at 5 ng/ml compared with control (Figure 8B). There was no difference in fibronectin nor periostin expression with TNF-α treatment.

Discussion

To the best of our knowledge, this is the first study to directly examine the molecular phenotype of myocardial fibrosis in LV heart tissue from donors with advanced CKD as well as its mechanisms and metabolism. We report that myocardial fibrosis in hearts from patients with advanced CKD is characterized by increased trimeric collagen type I, decreased collagen type III, and downregulation of cross-linking enzyme LOX and collagenases MMP1 and MMP2. All of the human hearts expressed only the trimeric form of collagen type I suggesting that collagen type I in human hearts is stabilized with intramolecular cross-links. It is possible that dimeric and monomeric forms of collagen are not present at significant amounts because they are already cross-linked in dense cardiac tissue versus cardiac fibroblast cell culture that can produce nascent collagen.

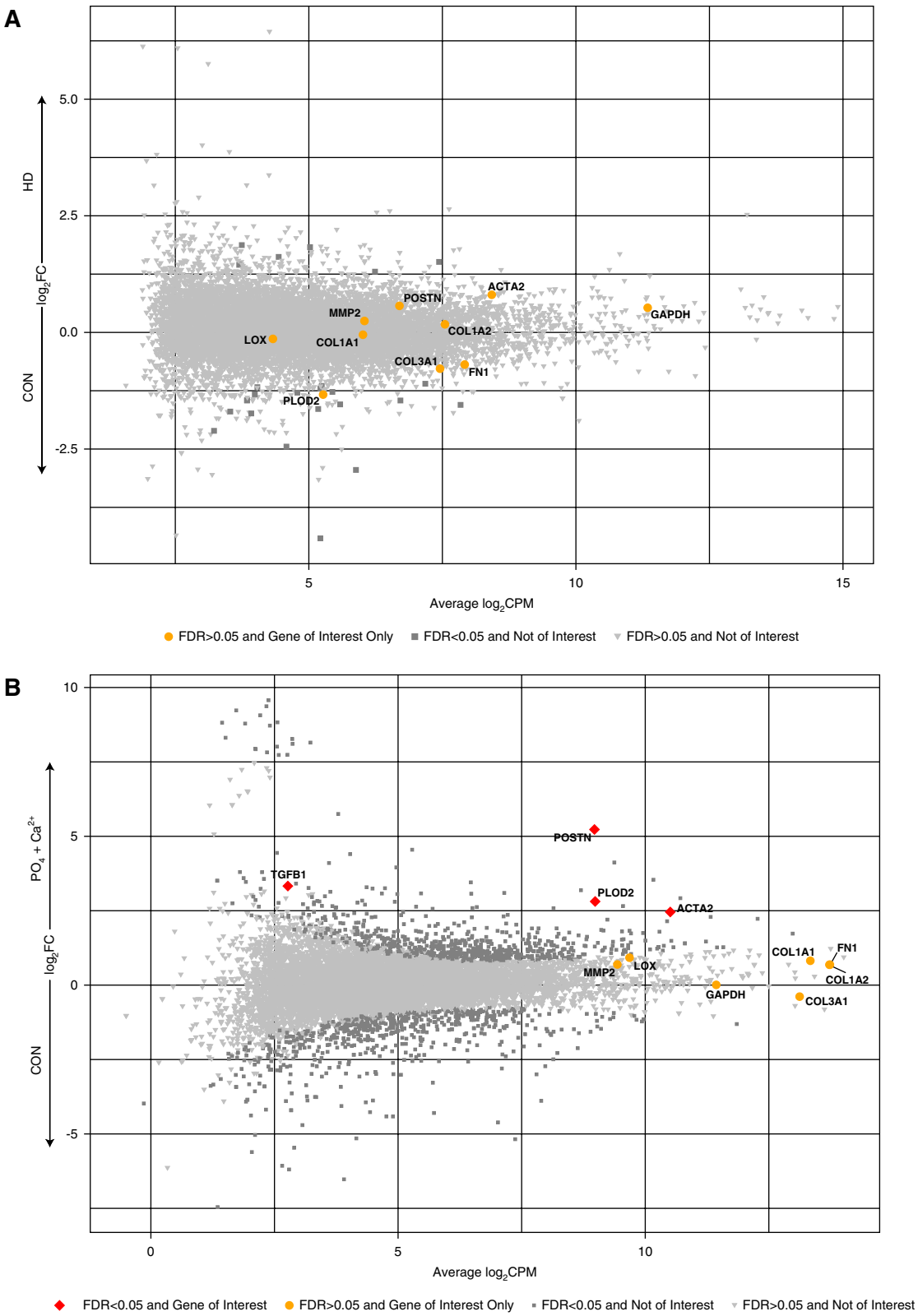

Figure 3. Differential gene expression analysis of human hearts and cardiac fibroblasts. (A) RNA-seq analysis of left ventricular human heart tissues from hemodialysis (HD, n=13) and healthy control (CON, n=4) hearts. Fibrosis-related genes of interest and reference genes are highlighted in red. There was no significant difference in expression of the genes of interest. Significantly differentially expressed genes (FDR<0.05) are shaped as triangular points versus circular points. (B) RNA-seq analysis human primary cardiac fibroblasts treated with 5 mM phosphate and 5 mM calcium (n=3) and 0.9 mM phosphate and 1.8 mM calcium controls (n=3). Fibrosis-related genes of interest and

Figure 3. *(Continued).* reference genes are highlighted in red. Significantly differentially expressed genes (*FDR*<0.05) are shaped as triangular points versus circular points. Periostin (POSTN), lysl hydroxylase 2 (PLOD2), TGF-β1 (TGFB1), and α-smooth muscle actin (ACTA2) were significantly upregulated in cardiac fibroblasts treated with high phosphate and high calcium. CPM, counts per million; FC, fold change.

Importantly, HD hearts exhibited increased trimeric collagen I compared with CON hearts, suggesting increased degradation-resistant, cross-linked collagen that can lead to ventricular stiffness and diastolic heart failure in advanced CKD. Given the lack of significant difference in collagen type I mRNA expression and in the proportion of total insoluble and soluble collagen in LV tissues between the three groups, the increased trimeric collagen type I may result primarily from decreased collagen degradation as explained by decreased MMP1 and MMP2 expression. The reliance of Sircol assay on acetic acid–pepsin digestion may exclude cross-linking occurring within the collagen

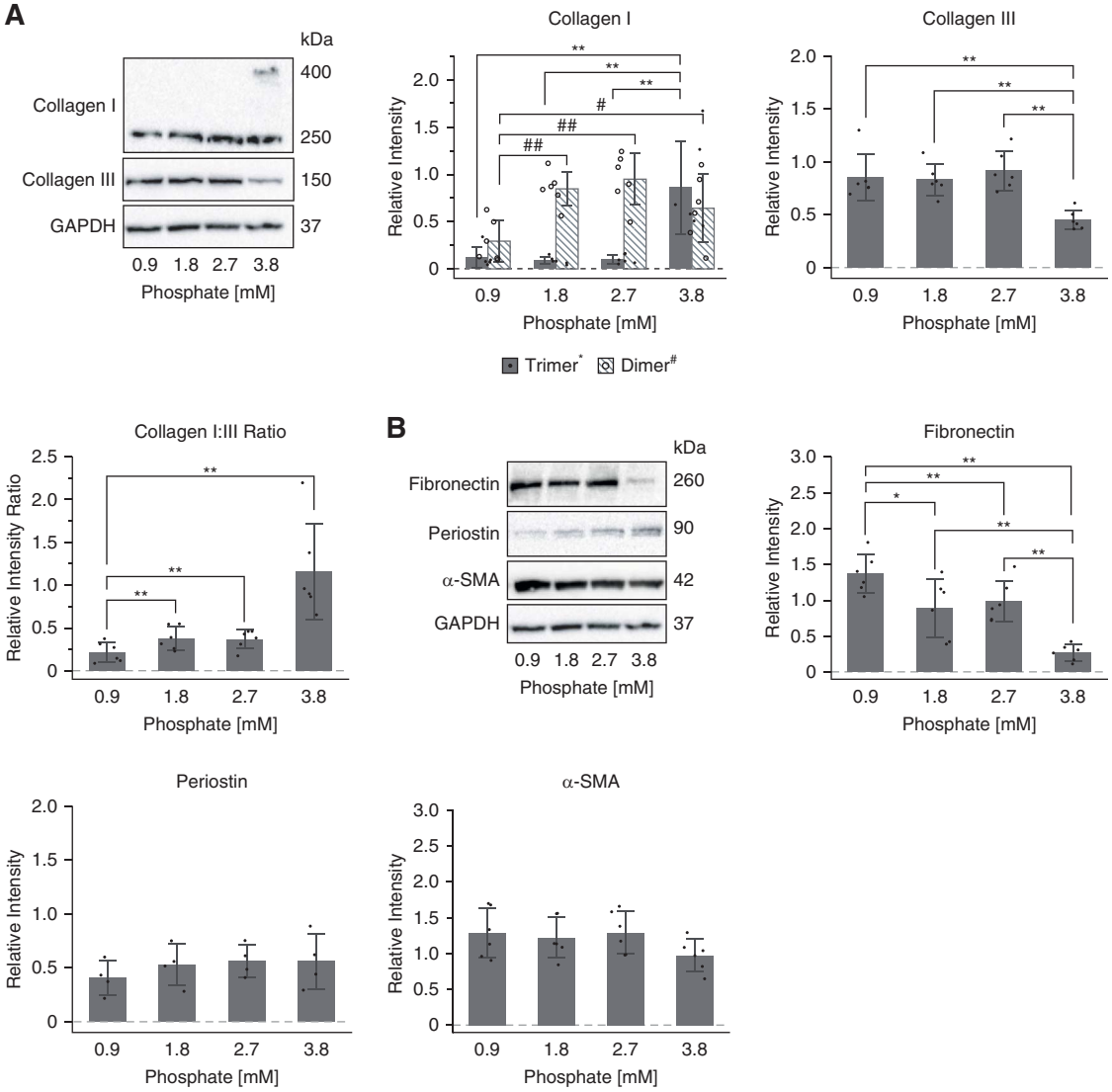

Figure 4. Elevated phosphate can induce trimerization of collagen type I and downregulate fibrillogenesis component, fibronectin, in cardiac fibroblasts. (A) Representative immunoblots of collagen type I, collagen type III, and GAPDH of cardiac fibroblasts treated with varying concentrations of β-glycerophosphate (n=6 each treatment). Trimeric collagen type I appears at 400 kDa and dimeric collagen type I appears at 250 kDa. 1.8 and 2.7 mM phosphate treatment exhibited significantly increased collagen type I dimer compared with 0.9 mM phosphate control levels. Trimeric collagen type I was significantly increased only at 3.8 mM phosphate compared with control. Collagen type III levels significantly decrease at 3.8 mM phosphate compared with 0.9 mM control. 2.7 and 3.8 mM phosphate treatment resulted in a higher collagen type I:III ratio compared with 0.9 mM control. (B) Representative immunoblots of fibronectin, periostin, α-SMA, and GAPDH of cardiac fibroblasts treated with varying concentrations of β-glycerophosphate (n=4–6). Fibronectin levels significantly decrease with an increase in phosphate levels compared with 0.9 mM control. There was no significant difference in periostin or α-SMA expression across all treatments. *P* values: * or # <0.05, ** or ## <0.01. Statistical significance was determined by one-way ANOVA and pairwise *t* test.

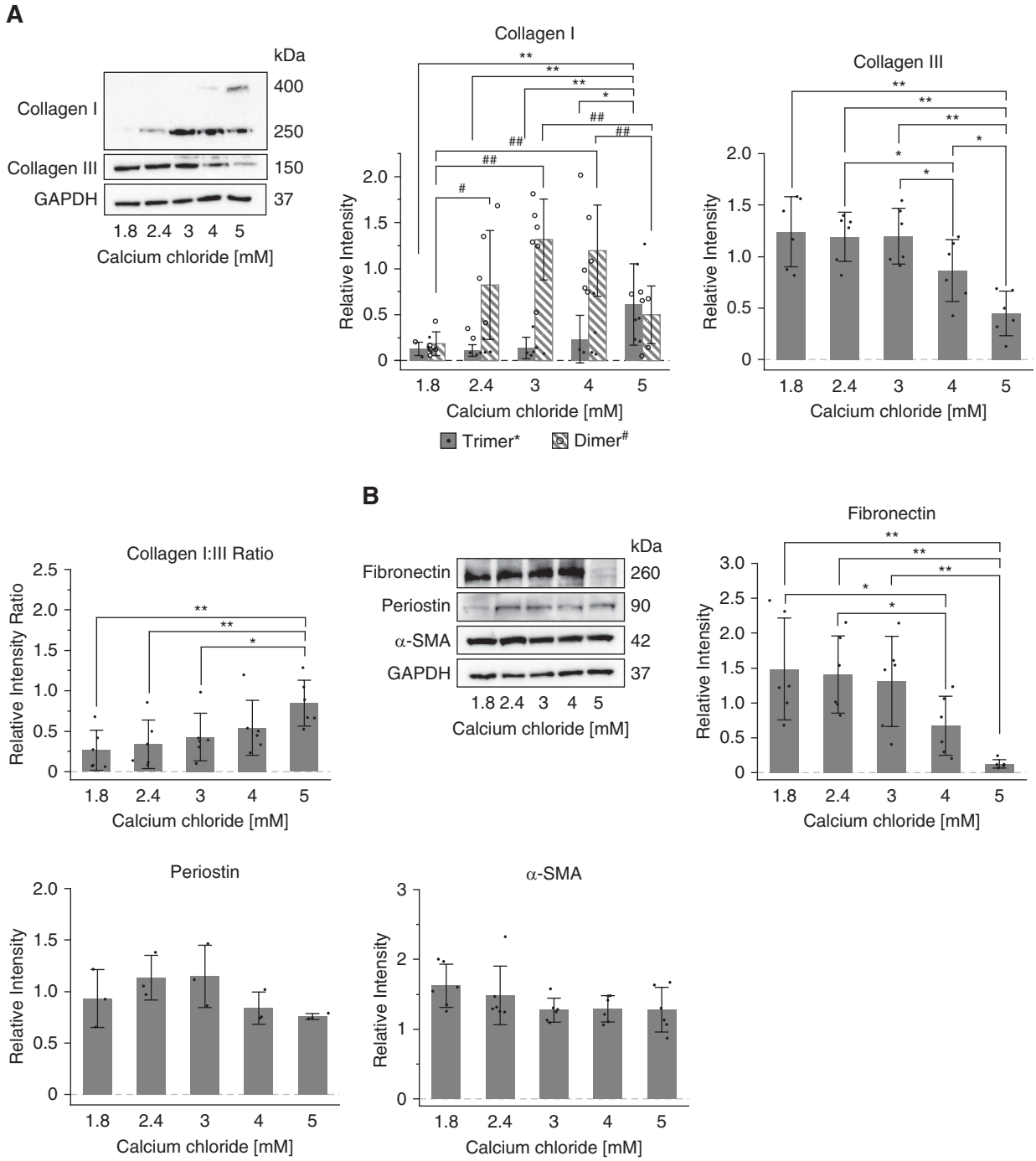

Figure 5. Elevated calcium can induce trimerization of collagen type I and downregulate fibrillogenesis component, fibronectin, in cardiac fibroblasts. (A) Representative immunoblots of collagen type I, collagen type III, and GAPDH of cardiac fibroblasts treated with varying concentrations of calcium chloride (n=6 each treatment). Trimeric collagen type I appears at 400 kDa and dimeric collagen type I appears at 250 kDa. 2.4, 3, and 4 mM calcium treatment exhibited significantly increased collagen type I dimer compared with 0.9 mM phosphate control levels. 5 mM calcium significantly increased collagen type I, decreased collagen type III, and overall increased collagen type I:III ratio compared with 0.9 mM control. (B) Representative immunoblots of fibronectin, periostin, α-smooth muscle actin (α-SMA), and GAPDH of cardiac fibroblasts treated with varying concentrations of calcium chloride (n=3–6). Fibronectin levels significantly decrease with elevated calcium levels at 4 and 5 mM compared with 0.9 mM control. There was no significant difference in periostin or α-SMA expression across all treatments. P values: * or # <0.05, ** or ## <0.01. Statistical significance determined by one-way ANOVA and pairwise t test.

telopeptides that is away from the pepsin cleavage site.[44] Therefore, it is possible that the assay is underestimating the total amount of cross-linked collagen and instead measuring only pepsin-insoluble collagen that is not significantly different across the three groups. Furthermore, the Sircol insoluble collagen assay cannot distinguish

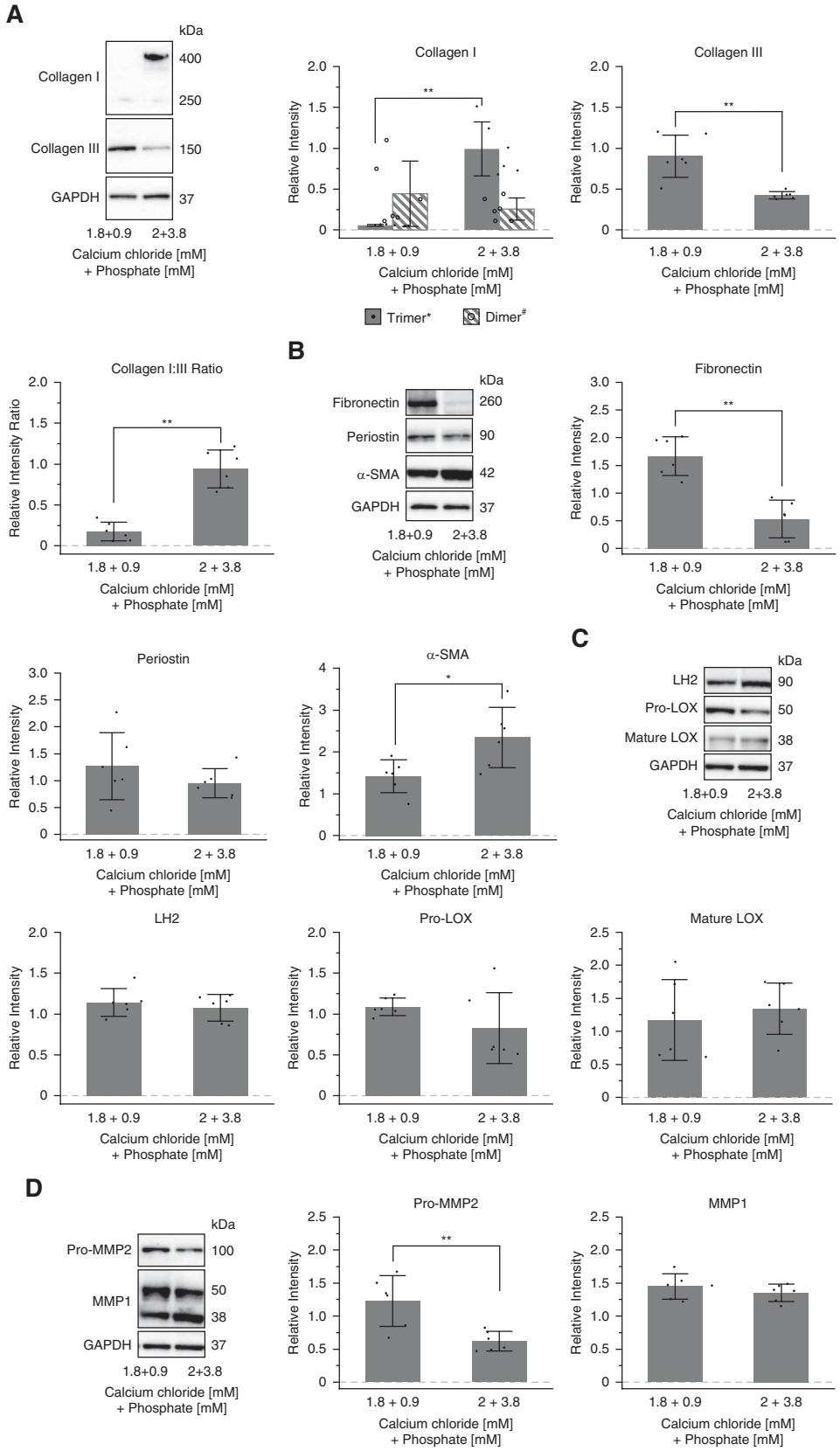

Figure 6. Mineral stressors promote intramolecular collagen cross-linking and fibrotic ratio of collagen type I:III while downregulating fibronectin and collagen turnover. (A) Representative immunoblots of collagen type I, collagen type III, and GAPDH of cardiac fibroblasts treated with combined calcium chloride and β-glycerophosphate totaling 2 mM calcium and 3.8 mM phosphate (n=6). Trimeric collagen type

Figure 6. *(Continued).* I appears at 400 kDa and dimeric collagen type I appears at 250 kDa. Combined elevated calcium and phosphate treatment significantly increased trimeric collagen type I, decreased collagen type III, and overall higher collagen type I:III ratio compared with 1.8 mM calcium and 0.9 mM phosphate control media. (B) Representative immunoblots of fibronectin, periostin, α-smooth muscle actin (α-SMA), and GAPDH of cardiac fibroblasts treated with combined calcium chloride and β-glycerophosphate totaling 2 mM calcium and 3.8 mM phosphate (n=6). Combined elevated calcium and phosphate treatment significantly decreased fibronectin and increased α-SMA compared with control. There was no significant difference in periostin expression. (C) Representative immunoblots of lysyl hydroxylase 2 (LH2), proenzyme lysyl oxidase (pro-LOX), proteolytically processed pro-LOX (mature LOX), and GAPDH of cardiac fibroblasts treated with combined calcium chloride and β-glycerophosphate totaling 2 mM calcium and 3.8 mM phosphate (n=6). There was no difference in cross-linking enzyme expression. (D) Representative immunoblots of metalloproteinase-1 (MMP1) and proenzyme metalloproteinase-2 (Pro-MMP2), and GAPDH of cardiac fibroblasts treated with combined calcium chloride and β-glycerophosphate totaling 2 mM calcium and 3.8 mM phosphate (n=6). Combined elevated calcium and phosphate treatment significantly decreased pro-MMP2 compared with control. There was no significant difference in MMP1 expression. P values: **<0.01. Statistical significance determined by one-way ANOVA and pairwise t test.

between types of cross-linking that may arise from the heterogeneous uremic environment in advanced CKD.[45–48] Fibrosis of the heart may be reflected better by the difference in types of cross-links present rather than an increase in total cross-links. This is seen in fibrosis of the skin, which is characterized by a shift from an allysine to a more degradation-resistant hydroxyallysine cross-link without a change in total cross-linking.[49] Hemodialysis hearts may also have more of a degradation-resistant cross-linking that could contribute to the increased trimeric collagen type I compared with hypertensive and healthy control hearts.

We found that mineral stressors including high calcium and phosphate found in CKD not only have a dose-dependent effect on increasing collagen type I in its dimeric form but also induce trimerization of collagen type I in cardiac fibroblasts. This is in contrast to profibrotic and proinflammatory cytokines, TGF-β and TNF-α, which increased dimeric collagen type I but did not induce collagen type I trimerization in cardiac fibroblasts. Mineral stressors also decreased zymogen collagenase MMP2 but not MMP1. Furthermore, mineral stressors did not significantly affect the expression of periostin, which promotes collagen cross-linking through collagen binding and LOX/LH2 activation.[38,50,51] Our results suggest that calcium and phosphate are directly involved in collagen intramolecular cross-linking into stable trimers and contribute to decreased collagen turnover. Calcium and phosphate ions can form nucleation sites for calcium-phosphate crystals that compact or stiffen the conformation of the collagen helices, which is conducive to inorganic cross-linking.[52–54] Pathologic excess of collagen cross-linking results in myocardial stiffness and decline in ventricular function, and inhibition of cross-linking enzymes can reduce tissue stiffness.[55,56] Therefore, these results suggest that tight control of mineral levels in the management of patients with advanced CKD may help reduce cross-linking that is associated with myocardial stiffness in advanced CKD.

In addition to collagen type I trimerization, hearts from hemodialysis donors exhibited a decrease in collagen type III compared with hearts from patients with hypertension and control donors, suggesting less tissue elasticity. Collagen type III can interact with collagen type I to form heterotypic collagen fibers that are more elastic than homotypic collagen type I fibers.[57,58] Decreased collagen III has been associated with reduced cardiac systolic function, which is restored with supplementation of collagen type III.[59] Cardiac fibroblasts treated with mineral stressors reflected a similar decline in collagen type III, whereas cardiac fibroblasts treated with TGF-β and TNF-α either exhibited an increased expression of collagen type III or had no significant effect. Reduction in elasticity and decreased collagen turnover are typical of an adverse fibrotic phenotype of the heart.[31,59,60] Our data suggest that mineral stressors induce a fibrotic phenotype distinct from fibrosis caused by hypertension or proinflammatory cytokines. This is further supported by our results demonstrating that phosphate and calcium induce a decrease in the fibrillogenic factor fibronectin, in contrast to an increase in fibronectin with cytokine treatment in cardiac fibroblasts. The insignificant difference in fibrillogenic factors in hemodialysis hearts compared with control may result from the combined countering effects of mineral stressors and profibrotic and proinflammatory cytokines. Fibronectin and integrins are essential to proper collagen fibril assembly.[61] However, mineral dysregulation may induce a fibronectin-independent but integrin-dependent mechanism for intramolecular collagen cross-linking.[62] In fact, collagen networks can assemble through integrins without fibronectin in remodeling adult liver cells after acute liver injury.[63] Our study emphasizes the distinct complexity of fibrosis in CKD-associated cardiomyopathy and caution in our approach to extrapolate findings from other models of myocardial fibrosis to the context of CKD. We recognize that diabetes mellitus is a major cause of CKD, which is reflected by the fact that 72% of the HD donors were diabetic. Diabetes may also contribute to the fibrotic phenotype in CKD through formation of advanced glycation end products in addition to mineral stressors and cytokines. The causal order of CKD-associated factors that contribute to the development of a fibrotic phenotype of the heart in advanced CKD is still largely unknown. We postulate that inflammation may prime the development of fibrosis in which mineral imbalance then triggers pathologic collagen deposition.

The results of this study should be interpreted against its limitations. First, there are multitudes of CKD-associated circulating risk factors and ECM components that may be involved in the development of cardiac fibrosis to varying degrees that cannot be studied in its entirety. In this study, we have selected to study major established circulating stress factors in uremia that have been associated with cardiac remodeling in CKD and major components of the ECM. Second, although our *in vitro* myocardial fibrosis model allows us to dissect the effects of individual

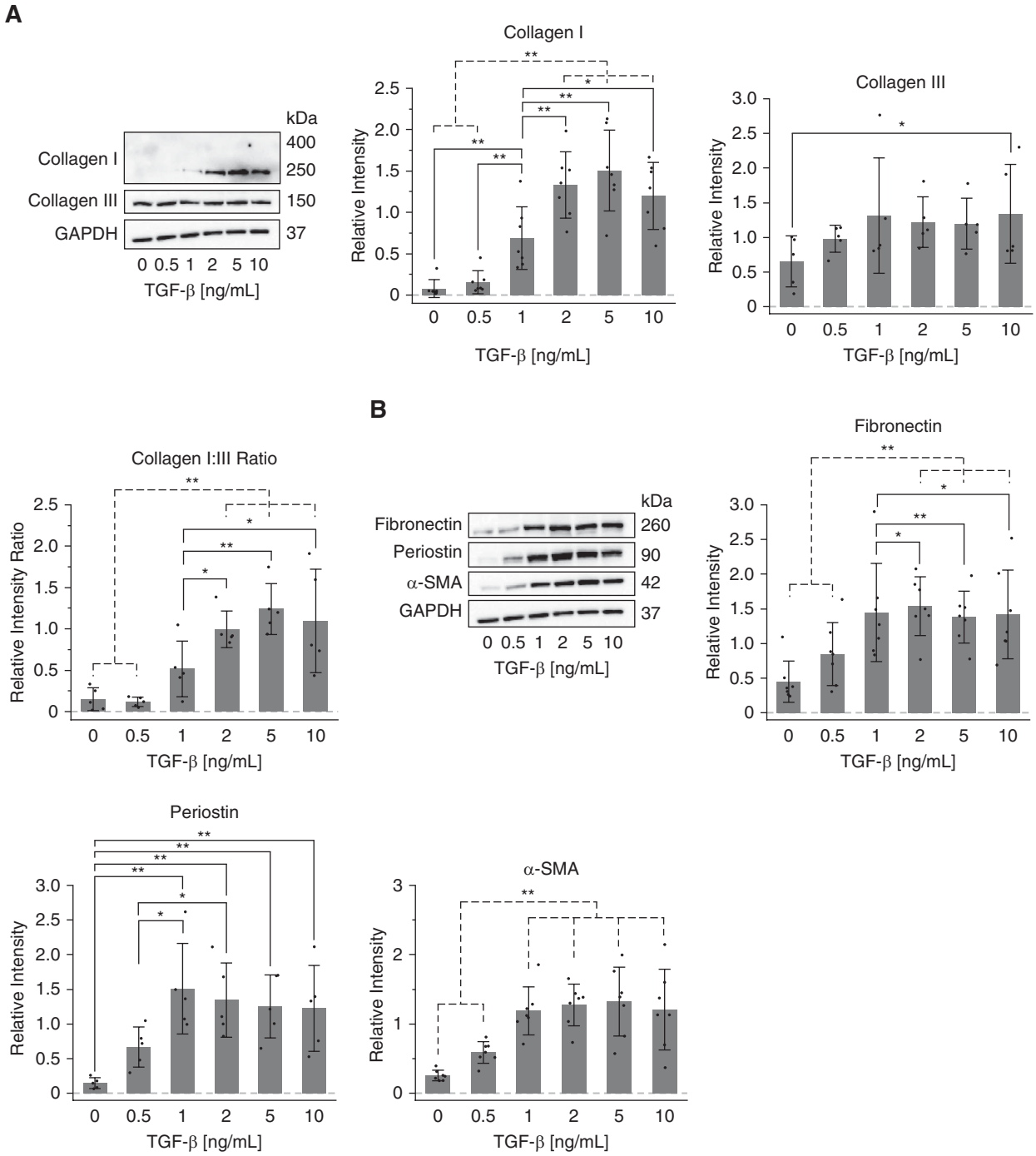

Figure 7. TGF-β increases production of both collagen types I and III and upregulates collagen fibrillogenesis. (A) Representative immunoblots of collagen type I, collagen type III, and GAPDH of cardiac fibroblasts treated with varying concentrations of TGF-β (n=5–7 each treatment). Only dimeric collagen type I (250 kDa) was observed. Increase in TGF-β led to an increase in dimeric collagen type I, collagen type III, and overall higher collagen type I:III ratio compared with control. (B) Representative immunoblots of fibronectin, periostin, α-SMA, and GAPDH of cardiac fibroblasts treated with varying concentrations of TGF-β (n=5–7). Increase in TGF-β led to a significant increase in fibronectin starting at 1 ng/ml compared with control. Increase in TGF-β also led to a significant increase in periostin and α-SMA starting at 0.5 ng/ml compared with control. P values: *<0.05, **<0.01. Statistical significance determined by one-way ANOVA and pairwise t test.

components of uremia, the model is limited by its single-cell nature. Finally, only a subset of HD (n=13) and CON (n=5) hearts were included in RNA-seq analysis because of either inadequate sample quality or technical batch effects, thereby rendering the results potentially nonconclusive. However, our study has several strengths including the utilization of a rare cohort of human hearts from patients with advanced CKD. Another strength of our study is the multi-arm–controlled design that allows us to distinguish cardiac changes resulting in advanced

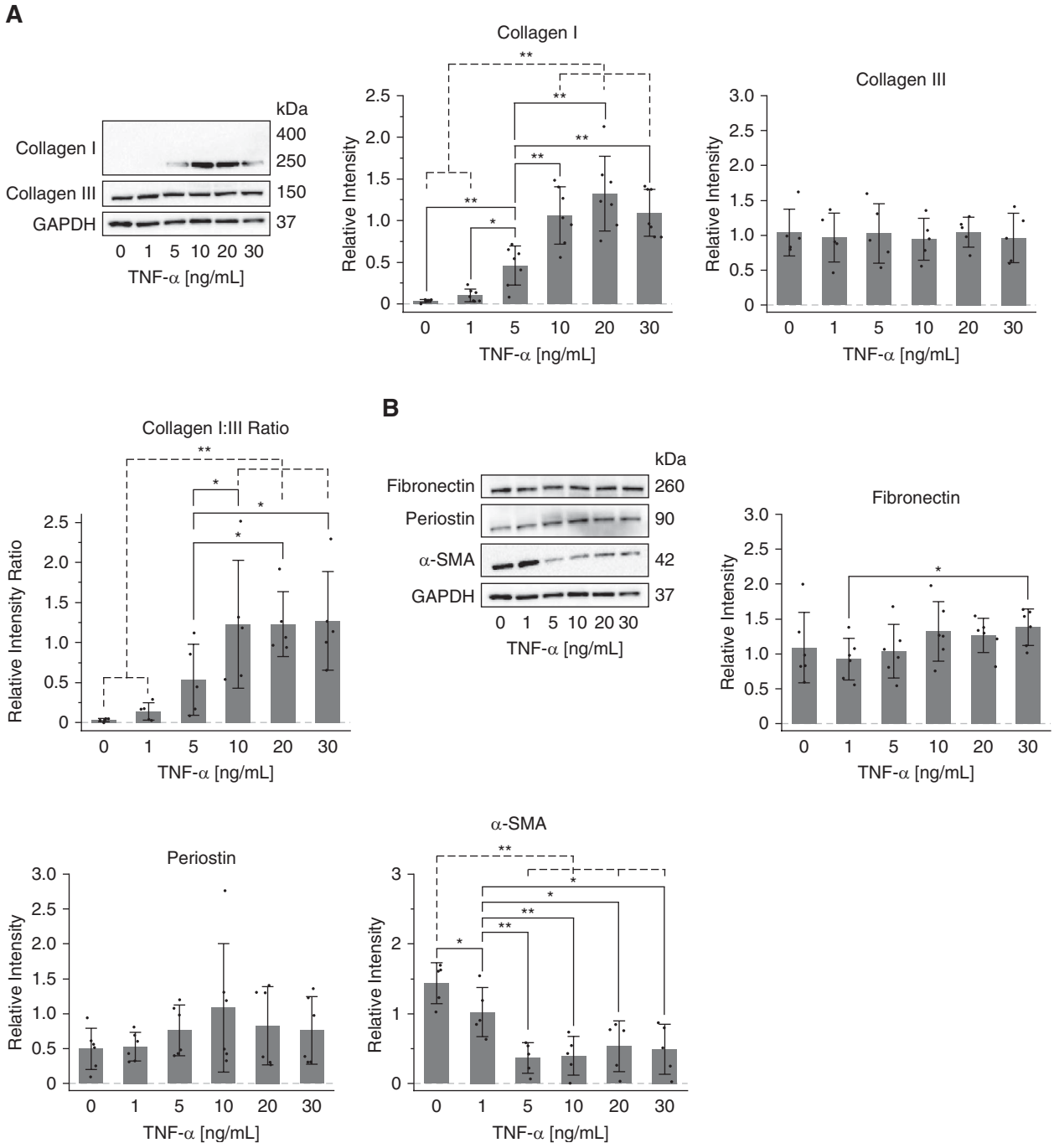

Figure 8. TNF-α selectively increased production of collagen type I but not type III with no effect on fibrillogenesis factors. (A) Representative immunoblots of collagen type I, collagen type III, and GAPDH of cardiac fibroblasts treated with varying concentrations of TNF-α (n=5–7 each treatment). Only dimeric collagen type I (250 kDa) was observed. Increase in TNF-α led to an increase in dimeric collagen type I and a higher collagen type I:III ratio without a significant change in collagen type III compared with control. (B) Representative immunoblots of fibronectin, periostin, α-SMA, and GAPDH of cardiac fibroblasts treated with varying concentrations of TNF-α (n=5–7). Increase in TNF-α led to a significant decrease in α-SMA starting at 5 ng/ml compared with control. There was a slight significant increase in fibronectin from 1 to 30 ng/ml TNF-α. There was no significant difference in periostin expression across all treatments. P values: *<0.05, **<0.01. Statistical significance determined by one-way ANOVA and pairwise t test.

CKD from those that occur from primarily hypertension, which is almost universally present in patients with CKD. Furthermore, this study is one of the few that provides transcriptomic profiling of genes associated with fibrogenesis in both human hearts and in single-cell culture and would be an important resource for future studies.

In conclusion, this study provides evidence that (*1*) myocardial fibrosis in patients with advanced CKD involves increased trimeric collagen type I expression along with

dysregulation of collagen turnover, (*2*) elevated levels of mineral stressors uniquely induce formation of intramolecularly cross-linked trimeric collagen in cardiac fibroblasts, (*3*) mineral stressors drive a fibronectin-independent mechanism of collagen fibrillogenesis, and (*4*) mineral imbalance and cytokines found in CKD drive different and distinct molecular profiles of fibrosis in cardiac fibroblasts. The findings from this study have furthered our understanding of myocardial fibrosis and revealed potential novel targets.

Disclosures

K. Lim reports consultancy agreements with Ambassadors Global and MBX Biosciences; ownership interest in OVIBIO Corporation, Ambassadors Global, and MBX Biosciences; advisory or leadership role in Ambassadors Global MBX Biosciences; and PI grant of Dialysis Clinics Inc (DCI) (Paul Teschan Research Fund (PTRF)), IU Health Values Fund Award. T. Lu reports ownership interest in Ovibio corporation, and CHF Foundation Funding Award. S. Moe reports consultancy agreements with Amgen, Ardelyx, Sanifit/Vifor, and Inozyme; ownership interest in Eli Lilly (stock); research funding from NIH-research grant and Keryx-research grant; honoraria from Ardelyx, Sanifit, and Inozyme; and advisory or leadership role in Editorial Board of AJ Nephrology and AJ Nutrition. G. Narayanan reports patents or royalties from Indiana University. A. Halim reports NIH NRSA Fellowship from NIH T32 AR065971, ownership interest in OVIBIO Corporation and patents or royalties from Indiana University. D. Zehnder reports research funding from Abbott Laboratories and Amgen and honoraria from Abbott Laboratories and Amgen. The remaining authors have nothing to disclose.

Funding

This work is supported by the National Institutes of Health from K23 DK115683-01, Ralph W. and Grace M. Showalter Research Trust Fund, Biomedical Research Grant from the Indiana Clinical and Translational Science Institute (CTSI) (K. Lim).

Acknowledgments

The content is solely the responsibility of the authors and does not necessarily represent the official views of the Showalter Research Trust or Indiana University School of Medicine.

Author Contributions

Conceptualization: Kenneth Lim, Sharon M. Moe.
Data curation: Arvin Halim, Takashi Hato, Kenneth Lim, Tzongshi Lu, Gayatri Narayanan.
Formal analysis: Arvin Halim, Takashi Hato, Tzongshi Lu, Gayatri Narayanan.
Funding acquisition: Kenneth Lim.
Investigation: Arvin Halim, Kenneth Lim, Tzongshi Lu, Gayatri Narayanan.
Methodology: Neal X. Chen, Arvin Halim, Takashi Hato, Kenneth Lim, Tzongshi Lu, Gayatri Narayanan.
Resources: Kenneth Lim, Sharon M. Moe, Daniel Zehnder.
Supervision: Kenneth Lim, Tzongshi Lu.
Validation: Neal X. Chen, Arvin Halim, Gayatri Narayanan.
Visualization: Arvin Halim, Kenneth Lim, Gayatri Narayanan.
Writing – original draft: Arvin Halim, Alvin Hu, Gayatri Narayanan.
Writing – review & editing: Keith G. Avin, Neal X. Chen, Takashi Hato, Alvin Hu, Kenneth Lim, Tzongshi Lu, Sharon M. Moe, Daniel Zehnder.

Data Sharing Statement

All data are included in the manuscript and/or supporting information. Previously published data were used for this study. Halim, Arvin et al. "Myocardial Cytoskeletal Adaptations in Advanced Kidney Disease." Journal of the American Heart Association vol. 11,5 (2022): e022991. doi:10.1161/JAHA.121.022991.

Supplemental Material

This article contains the following supplemental material online at http://links.lww.com/KN9/A398.

Supplemental Methods.
Supplemental Figure 1. Sircol soluble and insoluble collagen.
Supplemental Figure 2. FBS concentration experiments.

References

1. Romero-Gonzalez G, Gonzalez A, Lopez B, Ravassa S, Diez J. Heart failure in chronic kidney disease: the emerging role of myocardial fibrosis. *Nephrol Dial Transplant*. 2022;37(5):817–824. doi:10.1093/ndt/gfaa284
2. Hayer MK, Radhakrishnan A, Price AM, et al. Defining myocardial abnormalities across the stages of chronic kidney disease: a cardiac magnetic resonance imaging study. *JACC Cardiovasc Imaging*. 2020;13(11):2357–2367. doi:10.1016/j.jcmg.2020.04.021
3. Panizo S, Martinez-Arias L, Alonso-Montes C, et al. Fibrosis in chronic kidney disease: pathogenesis and consequences. *Int J Mol Sci*. 2021;22(1):408. doi:10.3390/ijms22010408
4. Edwards NC, Hayer MK, Ferro CJ, Townend JN, Steeds RP. CKD associated cardiomyopathy: molecular mechanisms, imaging modalities, disease evolution and interventions. In: Rangaswami J, Lerma EV, Ronco C, eds. *Cardio-Nephrology: Confluence of the Heart and Kidney in Clinical Practice*. Springer International Publishing; 2017:45–58.
5. Yamamoto K, Masuyama T, Sakata Y, et al. Myocardial stiffness is determined by ventricular fibrosis, but not by compensatory or excessive hypertrophy in hypertensive heart. *Cardiovasc Res*. 2002;55(1):76–82. doi:10.1016/s0008-6363(02)00341-3
6. Munch J, Abdelilah-Seyfried S. Sensing and responding of cardiomyocytes to changes of tissue stiffness in the diseased heart. *Front Cell Dev Biol*. 2021;9:642840. doi:10.3389/fcell.2021.642840
7. Conrad CH, Brooks WW, Hayes JA, Sen S, Robinson KG, Bing OH. Myocardial fibrosis and stiffness with hypertrophy and heart failure in the spontaneously hypertensive rat. *Circulation*. 1995;91(1):161–170. doi:10.1161/01.cir.91.1.161
8. Liu T, Song D, Dong J, et al. Current understanding of the pathophysiology of myocardial fibrosis and its quantitative assessment in heart failure. *Front Physiol*. 2017;8:238. doi:10.3389/fphys.2017.00238
9. Schelbert EB, Fridman Y, Wong TC, et al. Temporal relation between myocardial fibrosis and heart failure with preserved ejection fraction: association with baseline disease severity and subsequent outcome. *JAMA Cardiol*. 2017;2(9):995–1006. doi:10.1001/jamacardio.2017.2511
10. Verheule S, Schotten U. Electrophysiological consequences of cardiac fibrosis. *Cells*. 2021;10(11):3220. doi:10.3390/cells10113220
11. de Jong S, van Veen TA, van Rijen HV, de Bakker JM. Fibrosis and cardiac arrhythmias. *J Cardiovasc Pharmacol*. 2011;57(6):630–638. doi:10.1097/FJC.0b013e318207a35f
12. Schiau C, Leucuta DC, Dudea SM, Manole S. Myocardial fibrosis as a predictor of ventricular arrhythmias in patients with non-ischemic cardiomyopathy. *In Vivo*. 2021;35(3):1677–1685. doi:10.21873/invivo.12427
13. Wang J, Yang F, Wan K, Mui D, Han Y, Chen Y. Left ventricular midwall fibrosis as a predictor of sudden cardiac death in non-ischaemic dilated cardiomyopathy: a meta-analysis. *ESC Heart Fail*. 2020;7(5):2184–2192. doi:10.1002/ehf2.12865
14. Gulati A, Jabbour A, Ismail TF, et al. Association of fibrosis with mortality and sudden cardiac death in patients with nonischemic dilated cardiomyopathy. *JAMA*. 2013;309(9):896–908. doi:10.1001/jama.2013.1363

15. Biernacka A, Frangogiannis NG. Aging and cardiac fibrosis. *Aging Dis*. 2011;2:158–173. PMID: 21837283.
16. Sweeney M, Corden B, Cook SA. Targeting cardiac fibrosis in heart failure with preserved ejection fraction: mirage or miracle? *EMBO Mol Med*. 2020;12(10):e10865. doi:10.15252/emmm.201910865
17. Tian J, An X, Niu L. Myocardial fibrosis in congenital and pediatric heart disease. *Exp Ther Med*. 2017;13(5):1660–1664. doi:10.3892/etm.2017.4224
18. Hinderer S, Schenke-Layland K. Cardiac fibrosis—a short review of causes and therapeutic strategies. *Adv Drug Deliv Rev*. 2019;146:77–82. doi:10.1016/j.addr.2019.05.011
19. Kong P, Christia P, Frangogiannis NG. The pathogenesis of cardiac fibrosis. *Cell Mol Life Sci*. 2014;71(4):549–574. doi:10.1007/s00018-013-1349-6
20. Jiang W, Xiong Y, Li X, Yang Y. Cardiac fibrosis: cellular effectors, molecular pathways, and exosomal roles. *Front Cardiovasc Med*. 2021;8:715258. doi:10.3389/fcvm.2021.715258
21. Travers JG, Kamal FA, Robbins J, Yutzey KE, Blaxall BC. Cardiac fibrosis: the fibroblast awakens. *Circ Res*. 2016;118(6):1021–1040. doi:10.1161/CIRCRESAHA.115.306565
22. Rienks M, Papageorgiou AP, Frangogiannis NG, Heymans S. Myocardial extracellular matrix: an ever-changing and diverse entity. *Circ Res*. 2014;114(5):872–888. doi:10.1161/CIRCRESAHA.114.302533
23. Hortells L, Johansen AKZ, Yutzey KE. Cardiac fibroblasts and the extracellular matrix in regenerative and nonregenerative hearts. *J Cardiovasc Dev Dis*. 2019;6(3):29. doi:10.3390/jcdd6030029
24. Silva AC, Pereira C, Fonseca A, Pinto-do OP, Nascimento DS. Bearing my heart: the role of extracellular matrix on cardiac development, homeostasis, and injury response. *Front Cell Dev Biol*. 2020;8:621644. doi:10.3389/fcell.2020.621644
25. Wight TN, Potter-Perigo S. The extracellular matrix: an active or passive player in fibrosis? *Am J Physiol Gastrointest Liver Physiol*. 2011;301(6):G950–G955. doi:10.1152/ajpgi.00132.2011
26. Li L, Zhao Q, Kong W. Extracellular matrix remodeling and cardiac fibrosis. *Matrix Biol*. 2018;68-69:490–506. doi:10.1016/j.matbio.2018.01.013
27. MacKenna D, Summerour SR, Villarreal FJ. Role of mechanical factors in modulating cardiac fibroblast function and extracellular matrix synthesis. *Cardiovasc Res*. 2000;46(2):257–263. doi:10.1016/s0008-6363(00)00030-4
28. Frangogiannis NG. The extracellular matrix in ischemic and nonischemic heart failure. *Circ Res*. 2019;125(1):117–146. doi:10.1161/CIRCRESAHA.119.311148
29. Voorhees AP, DeLeon-Pennell KY, Ma Y, et al. Building a better infarct: modulation of collagen cross-linking to increase infarct stiffness and reduce left ventricular dilation post-myocardial infarction. *J Mol Cell Cardiol*. 2015;85:229–239. doi:10.1016/j.yjmcc.2015.06.006
30. Li YY, McTiernan CF, Feldman AM. Interplay of matrix metalloproteinases, tissue inhibitors of metalloproteinases and their regulators in cardiac matrix remodeling. *Cardiovasc Res*. 2000;46(2):214–224. doi:10.1016/s0008-6363(00)00003-1
31. Fan D, Takawale A, Lee J, Kassiri Z. Cardiac fibroblasts, fibrosis and extracellular matrix remodeling in heart disease. *Fibrogenesis Tissue Repair*. 2012;5(1):15. doi:10.1186/1755-1536-5-15
32. Turner NA, Porter KE. Regulation of myocardial matrix metalloproteinase expression and activity by cardiac fibroblasts. *IUBMB Life*. 2012;64(2):143–150. doi:10.1002/iub.594
33. Fields GB. Interstitial collagen catabolism. *J Biol Chem*. 2013;288(13):8785–8793. doi:10.1074/jbc.R113.451211
34. Lindner D, Zietsch C, Becher PM, et al. Differential expression of matrix metalloproteases in human fibroblasts with different origins. *Biochem Res Int*. 2012;2012:875742. doi:10.1155/2012/875742
35. Sottile J, Hocking DC. Fibronectin polymerization regulates the composition and stability of extracellular matrix fibrils and cell-matrix adhesions. *Mol Biol Cell*. 2002;13(10):3546–3559. doi:10.1091/mbc.e02-01-0048
36. Heling A, Zimmermann R, Kostin S, et al. Increased expression of cytoskeletal, linkage, and extracellular proteins in failing human myocardium. *Circ Res*. 2000;86(8):846–853. doi:10.1161/01.res.86.8.846
37. Valiente-Alandi I, Potter SJ, Salvador AM, et al. Inhibiting fibronectin attenuates fibrosis and improves cardiac function in a model of heart failure. *Circulation*. 2018;138(12):1236–1252. doi:10.1161/CIRCULATIONAHA.118.034609
38. Norris RA, Damon B, Mironov V, et al. Periostin regulates collagen fibrillogenesis and the biomechanical properties of connective tissues. *J Cell Biochem*. 2007;101(3):695–711. doi:10.1002/jcb.21224
39. Landry NM, Cohen S, Dixon IMC. Periostin in cardiovascular disease and development: a tale of two distinct roles. *Basic Res Cardiol*. 2018;113(1):1. doi:10.1007/s00395-017-0659-5
40. Zhao S, Wu H, Xia W, et al. Periostin expression is upregulated and associated with myocardial fibrosis in human failing hearts. *J Cardiol*. 2014;63(5):373–378. doi:10.1016/j.jjcc.2013.09.013
41. Halim A, Narayanan G, Hato T, et al. Myocardial cytoskeletal adaptations in advanced kidney disease. *J Am Heart Assoc*. 2022;11(5):e022991. doi:10.1161/JAHA.121.022991
42. Levey AS, Stevens LA, Schmid CH, et al. A new equation to estimate glomerular filtration rate. *Ann Intern Med*. 2009;150(9):604–612. doi:10.7326/0003-4819-150-9-200905050-00006
43. Valente MA, Hillege HL, Navis G, et al. The Chronic Kidney Disease Epidemiology Collaboration equation outperforms the Modification of Diet in Renal Disease equation for estimating glomerular filtration rate in chronic systolic heart failure. *Eur J Heart Fail*. 2014;16(1):86–94. doi:10.1093/eurjhf/hft128
44. Cundy TRR, Grey A. Chapter 31—metabolic bone disease. In: Marshall WJLM, Day AP, Ayling RM, ed. *Clinical Biochemistry: Metabolic and Clinical Aspects* (3rd ed). Churchill Livingstone; 2014:604–635.
45. Tenti P, Vannucci L. Lysyl oxidases: linking structures and immunity in the tumor microenvironment. *Cancer Immunol Immunother*. 2020;69(2):223–235. doi:10.1007/s00262-019-02404-x
46. Bastiaansen-Jenniskens YM, Koevoet W, De Bart AC, et al. TGFbeta affects collagen cross-linking independent of chondrocyte phenotype but strongly depending on physical environment. *Tissue Eng A*. 2008;14(6):1059–1066. doi:10.1089/ten.tea.2007.0345
47. Theiss AL, Simmons JG, Jobin C, Lund PK. Tumor necrosis factor (TNF) alpha increases collagen accumulation and proliferation in intestinal myofibroblasts via TNF receptor 2. *J Biol Chem*. 2005;280(43):36099–36109. doi:10.1074/jbc.M505291200
48. Lijnen P, Petrov V. Transforming growth factor-beta 1-induced collagen production in cultures of cardiac fibroblasts is the result of the appearance of myofibroblasts. *Methods Find Exp Clin Pharmacol*. 2002;24(6):333–344. doi:10.1358/mf.2002.24.6.693065
49. Brinckmann J, Neess CM, Gaber Y, et al. Different pattern of collagen cross-links in two sclerotic skin diseases: lipodermatosclerosis and circumscribed scleroderma. *J Invest Dermatol*. 2001;117(2):269–273. doi:10.1046/j.0022-202x.2001.01414.x
50. Kumar P, Smith T, Raeman R, et al. Periostin promotes liver fibrogenesis by activating lysyl oxidase in hepatic stellate cells. *J Biol Chem*. 2018;293(33):12781–12792. doi:10.1074/jbc.RA117.001601
51. Wietecha MS, Pensalfini M, Cangkrama M, et al. Activin-mediated alterations of the fibroblast transcriptome and matrisome control the biomechanical properties of skin wounds. *Nat Commun*. 2020;11(1):2604. doi:10.1038/s41467-020-16409-z
52. Cui FZ, Wang Y, Cai Q, Zhang W. Conformation change of collagen during the initial stage of biomineralization of calcium phosphate. *J Mater Chem*. 2008;18(32):3835–3840. doi:10.1039/B805467C
53. Zhang W, Huang Z-L, Liao S-S, Cui F-Z. Nucleation sites of calcium phosphate crystals during collagen mineralization. *J Am Ceram Soc*. 2003;86(6):1052–1054. doi:10.1111/j.1151-2916.2003.tb03422.x
54. Pang X, Lin L, Tang B. Unraveling the role of calcium ions in the mechanical properties of individual collagen fibrils. *Sci Rep*. 2017;7:46042. doi:10.1038/srep46042
55. Bi X, Song Y, Song Y, et al. Collagen cross-linking is associated with cardiac remodeling in hypertrophic obstructive

cardiomyopathy. *J Am Heart Assoc*. 2021;10(1):e017752. doi:10.1161/JAHA.120.017752
56. Neff LS, Bradshaw AD. Cross your heart? Collagen cross-links in cardiac health and disease. *Cell Signal*. 2021;79:109889. doi:10.1016/j.cellsig.2020.109889
57. Kitamura M, Shimizu M, Ino H, et al. Collagen remodeling and cardiac dysfunction in patients with hypertrophic cardiomyopathy: the significance of type III and VI collagens. *Clin Cardiol*. 2001;24(4):325–329. doi:10.1002/clc.4960240413
58. Parkin JD, San Antonio JD, Persikov AV, et al. The collαgen III fibril has a "flexi-rod" structure of flexible sequences interspersed with rigid bioactive domains including two with hemostatic roles. *PLoS One*. 2017;12(7):e0175582. doi:10.1371/journal.pone.0175582
59. Uchinaka A, Yoshida M, Tanaka K, et al. Overexpression of collagen type III in injured myocardium prevents cardiac systolic dysfunction by changing the balance of collagen distribution. *J Thorac Cardiovasc Surg*. 2018;156(1):217–226.e3. doi:10.1016/j.jtcvs.2018.01.097
60. Marijianowski MM, Teeling P, Mann J, Becker AE. Dilated cardiomyopathy is associated with an increase in the type I/type III collagen ratio: a quantitative assessment. *J Am Coll Cardiol*. 1995;25(6):1263–1272. doi:10.1016/0735-1097(94)00557-7
61. Kadler KE, Hill A, Canty-Laird EG. Collagen fibrillogenesis: fibronectin, integrins, and minor collagens as organizers and nucleators. *Curr Opin Cell Biol*. 2008;20(5):495–501. doi:10.1016/j.ceb.2008.06.008
62. Musiime M, Chang J, Hansen U, Kadler KE, Zeltz C, Gullberg D. Collagen assembly at the cell surface: Dogmas revisited. *Cells*. 2021;10(3):662. doi:10.3390/cells10030662
63. Moriya K, Bae E, Honda K, et al. A fibronectin-independent mechanism of collagen fibrillogenesis in adult liver remodeling. *Gastroenterology*. 2011;140(5):1653–1663. doi:10.1053/j.gastro.2011.02.005

Received: February 25, 2023 **Accepted:** October 11, 2023
Published Online Ahead of Print: October 20, 2023

See related editorial, "Insights into Myocardial Fibrosis in Advanced Chronic Kidney Disease Using Human Tissue," on pages 1531–1533.